

# Search for tetraquark candidate $Z(4430)$ in meson photoproduction

Xiao-Hai Liu<sup>1</sup> and Qiang Zhao<sup>1,2</sup>

1) *Institute of High Energy Physics, Chinese Academy of Sciences, Beijing 100049, P.R. China and*  
 2) *Department of Physics, University of Surrey, Guildford, GU2 7XH, United Kingdom*

Frank E. Close

*Rudolf Peierls Centre for Theoretical Physics, University of Oxford,  
 Keble Rd., Oxford, OX1 3NP, United Kingdom*

(Dated: June 16, 2018)

We propose a search for the newly discovered tetraquark candidate  $Z(4430)$  in photoproduction. Based on the Belle results we show that if  $Z(4430)$  is a genuine resonance, its significantly large coupling to  $\psi'\pi$  will cause it to stand out above the background in  $\gamma p \rightarrow Z^+(4430)n \rightarrow \psi'\pi^+n$ . We consider the dependence of the cross section for the quantum numbers ( $J^P = 1^-, 1^+$  or  $0^-$ ).

## I. INTRODUCTION

A resonant structure in the invariant mass of  $\psi'\pi^+$  at 4.43 GeV with a width of 45 MeV was recently reported by Belle in  $B \rightarrow K\psi'\pi$  [1]. This result immediately provoked much interest from experiment and theory due to the possibility of it being a tetraquark candidate [2, 3, 4, 5, 6] with flavor  $c\bar{c}u\bar{d}$  or  $c\bar{c}d\bar{u}$ , i.e. a charmonium with isospin  $I = 1$ .

It has also been proposed that this structure may be due to subthreshold effects in  $D^*\bar{D}_1$  rescattering [7, 8, 9, 10, 11]. Similar to the  $X(3872)$  which is proposed to be a possible bound state of  $D\bar{D}^*$  due to long-range  $\pi$  exchange forces [12, 13, 14], such a mechanism will favor  $J^P = 0^-, 1^-$  or  $2^-$  for  $Z(4430)$  with  $I = 1$  [11]. Also, it has been suggested by Maiani *et al.* [4] that the strong coupling of the  $Z(4430)$  to  $\psi'\pi$  instead of  $J/\psi\pi$  could be a signal for a radially excited  $1^{+-}$  tetraquark. Long ago Close and Lipkin [15] proposed that  $c\bar{c} + \pi$  is a channel that could identify tetraquark states such as  $1^{+-}$  in S-wave or, most interesting,  $1^{--}$  in P-wave, hence we shall also consider that  $Z(4430) \rightarrow \psi'\pi$  occurs via P-wave transition if it has  $J^{PC} = 1^{--}$ . In particular, a large coupling to  $\psi'\pi$  will have special implications for its photoproduction rate, and information about its quantum numbers may be extracted.

Seeing this state in an independent production process will be essential for establishing its existence and determining its nature. We propose here to look for the  $Z(4430)$  in photoproduction. If  $Z(4430)$  is a genuine signal for a tetraquark state which couples to  $\psi'\pi$ , then it can necessarily be photoproduced via  $\pi$  exchange through the  $\gamma - \psi'$  intermediate coupling. It suggests that  $\gamma p \rightarrow Z^+(4430)n \rightarrow \psi'\pi^+n$  could be a dominant production mechanism for  $Z(4430)$ . Therefore, by looking for the signal of  $Z(4430)$  in  $\gamma p \rightarrow Z^+(4430)n \rightarrow \psi'\pi^+n$ , one may establish this state as a genuine resonance. We also estimate a possible destructive interference from the intermediate  $\gamma - J/\psi$  coupling. Although Belle does not see the decay of  $Z(4430) \rightarrow J/\psi\pi$ , which implies a weaker  $ZJ/\psi\pi$  coupling, the relatively larger leptonic width for  $J/\psi \rightarrow e^+e^-$  than  $\psi' \rightarrow e^+e^-$  may still lead to sizeable contributions from intermediate  $J/\psi$  in photoproduction. We will investigate such effects in a vector meson dominance (VMD) model.

In addition, we consider background contributions to this channel which involve Pomeron exchanges and nucleon Born terms. Interestingly, this shows that these backgrounds have rather small interferences with the  $Z^+(4430)$  production. This enhances the possibility of identifying or refuting this state in photoproduction. Experimental data from DESY may be able to clarify this directly.

In the following we first provide a detailed description of the theoretical model by considering  $Z(4430)$  to have either  $J^P = 1^-, 1^+$  or  $0^-$ . The model predictions for the differential and total cross sections will be presented. We then make a quantitative analysis of the possible background contributions to  $\psi'\pi N$  final state. Dalitz plot analysis will be provided.

## II. THE MODEL

The production of  $Z^+$  in  $\gamma p \rightarrow Z^+ n$  can be described by the processes in Fig. 1. Its production possesses different features at different kinematics. We outline those features below as they are essential for constructing the theoretical model:

I) In the  $t$ -channel, as the electromagnetic (EM) interaction does not conserve isospin, the  $Z(4430)$  can be produced by either isoscalar or isovector exchange. Taking into account the flavor content, i.e.  $Z^+$  has a hidden  $c\bar{c}$  which does not carry isospin, the isoscalar exchange in the  $t$ -channel will be forbidden for the charged  $Z(4430)$  while suppressed for the neutral partner. We will come back to this point later.

Furthermore, as the  $Z(4430)$  has only been seen in the  $\psi'\pi$  channel, we shall concentrate on the  $t$ -channel pion exchange as a leading contribution. We shall argue that this is likely to give a lower limit for the photoproduction cross section. We note in advance that the inclusion of e.g.  $a_0$  exchange will increase the cross sections since there is no interferences between the pion and  $a_0$  exchange amplitudes. We will present some numerical estimates for the  $a_0(980)$  exchange later. Heavier  $t$ -channel meson (Regge) exchanges contribute to the cross section at off-forward angles and could become important in the higher energy region. As we do not have information about their couplings to  $Z(4430)\psi'$ , we shall focus on the near-threshold region where the dominant pion exchange can be well-constrained and reliably estimated.

II) For  $J^P = 1^-$  and  $0^-$ ,  $Z(4430)$  will couple to  $VP$  in  $P$ -wave at leading order, while for  $J^P = 1^+$ , it is via  $S$ -wave. We apply different effective Lagrangians to describe the  $Z\psi'\pi$  vertex.

III) There is no available information about the coupling for a  $Z$  to nucleons. This will appear in the  $s$  or  $u$ -channel where  $Z(4430)$  can directly couple to  $p$  and  $n$ . The  $s$ -channel process generally becomes important near threshold, and at middle and backward scattering angles. With increasing energies, these contributions die out quickly due to the suppression of the  $s$  and  $u$ -channel propagators and the effects of the nucleon's form factors. In contrast, the  $t$ -channel pion exchange may remain dominant at forward angles and give the major contribution to the cross section.

Based on the above rather general considerations, we identify processes that will drive the  $Z(4430)$  production. As the  $Z(4430)$  is observed to couple strongly to  $\psi'\pi$ , we propose to look for signals in  $\gamma p \rightarrow Z^+(4430)n \rightarrow \psi'\pi^+n$ , and  $\gamma p \rightarrow Z^0(4430)p \rightarrow \psi'\pi^0p$ . This gives rise to some background contributions as shown in Fig. 2, in particular, in the neutral  $Z(4430)$  production.

IV) As the  $Z(4430)$  is observed to couple to  $\psi'\pi$ , we derive the  $Z\gamma\pi$  coupling by Vector Meson Dominance (VMD), and assume that the  $Z\gamma\pi$  coupling is due to a sum of intermediate vector mesons which connect the photon with the  $Z(4430)$  and the exchanged  $\pi$ . We initially assume that  $\psi'$  is the dominant intermediate vector meson in the  $Z\gamma\pi$  coupling, and then consider the possible effect of a coupling to  $J/\psi\pi$ .

### A. Production of $Z(4430)$ with $J^P = 1^-$

For  $J^P = 1^-$ , the following Lagrangian is applied for the  $Z\psi'\pi$  coupling, e.g. for the charged  $Z(4430)$ ,

$$\mathcal{L}_{Z\psi'\pi} = \frac{g_{Z\psi'\pi}}{M_Z} \varepsilon_{\mu\nu\alpha\beta} \partial^\mu \psi'^\nu \partial^\alpha Z^{+\beta} \pi^- + H.c. , \quad (1)$$

where  $\varepsilon_{\mu\nu\alpha\beta}$  is Levi-Civita tensor, and the coupling constant  $g_{Z\psi'\pi}$  will be determined by the width  $\Gamma_{Z^\pm \rightarrow \psi'\pi^\pm}$  [1], i.e.

$$\Gamma_{Z \rightarrow \psi'\pi} = \frac{1}{8\pi} \frac{|\mathcal{M}|^2}{3} \frac{|\mathbf{p}_{\pi cm}|}{M_Z^2} , \quad (2)$$

where

$$\begin{aligned} |\mathcal{M}|^2 &= \left( \frac{g_{Z\psi'\pi}}{M_Z} \right)^2 [2(p_Z \cdot p_{\psi'})^2 - 2p_Z^2 p_{\psi'}^2] \\ &= \left( \frac{g_{Z\psi'\pi}}{M_Z} \right)^2 \left[ \frac{(M_Z^2 + M_{\psi'}^2 - m_\pi^2)^2}{2} - 2M_Z^2 M_{\psi'}^2 \right] , \end{aligned} \quad (3)$$

and  $\mathbf{p}_{\pi cm}$  is the three-vector momentum of the pion in the  $Z$  meson rest frame. With  $M_Z = 4433$  MeV, and  $\Gamma_{Z \rightarrow \psi' \pi} = 45$  MeV, we have  $g_{Z\psi'\pi}/M_Z = 2.365$  GeV $^{-1}$ . Any coupling to  $J/\psi\pi$  will be analogously related to  $g_{ZJ/\psi\pi}/M_Z$ , which in turn is driven by the (as yet unobserved) decay  $Z \rightarrow J/\psi\pi$ .

For the meson coupling vertices, we apply a form factor as follows:

$$F_Z = \frac{M_{\psi'}^2 - m_i^2}{M_{\psi'}^2 - q^2} \quad (4)$$

with  $m_i = m_\pi$ , and the cutoff is set as the mass of the intermediate vector meson [16], i.e.  $\Lambda = M_{\psi'}$ .

The general expression for an intermediate-vector-meson  $V$  coupling to  $\gamma$  at leading order is

$$\mathcal{L}_{V\gamma} = \frac{eM_V^2}{f_V} V_\mu A^\mu \quad (5)$$

the coupling constant  $e/f_V$  can be determined by  $V \rightarrow e^+e^-$ ,

$$\frac{e}{f_V} = \left[ \frac{3\Gamma_{V \rightarrow e^+e^-}}{2\alpha_e |p_e|} \right]^{1/2}, \quad (6)$$

where  $|p_e|$  is the electron three-moment in the vector meson rest frame, and  $\alpha_e = 1/137$  is the EM fine-structure constant. With  $\Gamma_{\psi' \rightarrow e^+e^-} = 2.48 \pm 0.06$  keV [17], it gives  $e/f_{\psi'} = 0.0166$ .

The  $\gamma$ - $J/\psi$  coupling analogously is  $e/f_{J/\psi} = 0.027$ . As this is larger than for the  $\psi'$  it is possible that any coupling  $Z \rightarrow J/\psi\pi$  could cause an additional contribution to the photoproduction amplitude, which could destructively interfere with the former and hence give a much reduced cross section. If this were the case, it would also imply that a branching ratio  $Z \rightarrow J/\psi\pi$  should be visible. We shall discuss the dependence of the photoproduction cross section on this.

At the meson nucleon coupling vertices we adopt the commonly used Lagrangian

$$\begin{aligned} \mathcal{L}_{\pi NN}^{int} &= -ig_{\pi NN} \bar{N} \gamma_5 (\vec{\tau} \cdot \vec{\pi}) N \\ &= -ig_{\pi NN} (\bar{p} \gamma_5 p \pi^0 + \sqrt{2} \bar{p} \gamma_5 n \pi^+ + \sqrt{2} \bar{n} \gamma_5 p \pi^- - \bar{n} \gamma_5 n \pi^0), \end{aligned} \quad (7)$$

where a standard value,  $g_{\pi NN}^2/4\pi = 14$ , is adopted [18]. In addition, a form factor is applied for the  $\pi NN$  vertex,

$$F_{\pi NN} = \frac{\Lambda_\pi^2 - m_\pi^2}{\Lambda_\pi^2 - q^2}, \quad (8)$$

with  $\Lambda_\pi = 0.7$  GeV. We note that this form factor successfully accounts for the photoproduction of  $\omega$  and  $\rho$  meson near threshold [16, 19]. Some works have argued for a larger value [20]. Such values would increase the cross sections relative to what we compute here, and so we use the cited value in the spirit of seeking a lower limit for the cross-section.

The effective Lagrangian leads to the amplitude for producing a charged  $Z(4430)$  via charged pion exchange in  $\gamma p \rightarrow Z^+(4430)n$ :

$$\begin{aligned} T_{1fi} &= -i \left( \sqrt{2} g_{\pi NN} \frac{g_{Z\psi'\pi}}{M_Z} \frac{e}{f_{\psi'}} \right) \bar{u}(p_2) \gamma_5 u(p_1) \varepsilon_{\mu\nu\alpha\beta} k_1^\mu k_2^\alpha \epsilon^\nu \epsilon_Z^{*\beta} \\ &\quad \times \frac{1}{q^2 - m_\pi^2} F_{\pi NN}(q^2) F_{Z\psi'\pi}(q^2), \end{aligned} \quad (9)$$

where  $p_1$  ( $k_1$ ) and  $p_2$  ( $k_2$ ) are four-vector momenta of initial nucleon (photon), and final nucleon ( $Z$  meson), respectively;  $\epsilon^\mu$  and  $\epsilon_Z^{*\beta}$  are the polarization vectors of  $\gamma$  and  $Z$ , respectively.

By defining  $t \equiv (p_1 - p_2)^2 \equiv q^2$ ,  $s \equiv (k_1 + p_1)^2$ , the differential cross section is

$$\frac{d\sigma}{dt} = \frac{1}{64\pi s} \frac{1}{|k_{1cm}|^2} \frac{1}{4} |\mathcal{M}|^2, \quad (10)$$

where the invariant matrix element squared gives

$$\begin{aligned}
|\mathcal{M}|^2 &= \sum_{pol} |T_{1fi}|^2 \\
&= \left( \sqrt{2} g_{\pi NN} \frac{g_{Z\psi'\pi}}{M_Z} \frac{e}{f_{\psi'}} \right)^2 \frac{-q^2(q^2 - M_Z^2)^2}{(q^2 - m_\pi^2)^2} \left( \frac{\Lambda_\pi^2 - m_\pi^2}{\Lambda_\pi^2 - q^2} \right)^2 \left( \frac{M_{\psi'}^2 - m_\pi^2}{M_{\psi'}^2 - q^2} \right)^2.
\end{aligned} \tag{11}$$

After integrating over the range of  $|t|$ , i.e. within  $t_{max}$  and  $t_{min}$ ,

$$t_{max}(t_{min}) = \frac{M_Z^4}{4s} - (k_{1cm} \mp k_{2cm})^2 \tag{12}$$

the total cross section can be obtained. In the above equation,  $k_{1cm} = \frac{E_\gamma M_N}{\sqrt{s}}$  is the photon energy in the overall c.m. system, where  $E_\gamma$  is the photon energy in the rest-frame of the initial proton.

In the Appendix, we provide the analogous expressions for  $t$ -channel  $a_0$  exchange. Note that the pion and  $a_0$  exchanges contribute to the real and imaginary part of the transition amplitude respectively. Thus, there are no interferences between these two channels, and the inclusion of the  $a_0$  exchange will enhance the  $Z(4430)$  cross section. As we lack knowledge on the  $Z\psi'a_0$  and  $a_0NN$  coupling strengths, which are in any event expected to be much smaller than the  $\pi$  exchange contributions, we will focus on the pion exchange here.

For neutral  $Z$  production contributions may also be allowed from Pomeron exchange. However, we argue that this scenario is suppressed due to the following reasons: i) In the case where the photon (isoscalar component) couples to  $c\bar{c}$ , isospin has to be transferred to the pair of light  $q\bar{q}$  in order to form  $Z^0(4430)$ . ii) The photon can couple to isovector vector mesons made of light  $q\bar{q}$ , which then pull out a pair of  $c\bar{c}$  after exchanging a Pomeron. Although this process conserves isospin, it is suppressed by the soft creation of a large mass  $c\bar{c}$ , and also as it requires the  $Z$  meson to be formed with the  $q\bar{q}$  and  $c\bar{c}$  pairs at relatively large momentum transfers. Consequently suppression from the final state wavefunction is likely. Precise estimates will be model dependent but for the purpose of estimating a lower limit for the production cross section, we neglect this contribution here.

In contrast, Pomeron contributions can generate background. As shown in Fig. 2(a) and (b), the direct production of  $\psi'$  allows Pomeron exchanges as an important production mechanism. An intermediate nucleon will then decay into a pion and nucleon. In principle, all the intermediate isospin 1/2 nucleon resonances can contribute to this process. Again, as a simple estimate of the background, we only consider the nucleon pole contributions.

### B. Production of $Z(4430)$ with $J^P = 1^+$

For the production of  $Z(4430)$  with  $J^P = 1^+$ , the difference from  $J^{PC} = 1^-$  is at the  $Z\psi'\pi$  vertex for which the following effective Lagrangian is adopted [21, 22]:

$$\mathcal{L}_{Z\psi'\pi} = \frac{g_{Z\psi'\pi}}{M_Z} (\partial^\alpha \psi'^\beta \partial_\alpha \pi Z_\beta - \partial^\alpha \psi'^\beta \partial_\beta \pi Z_\alpha), \tag{13}$$

where the notations are the same as Eq. (1). Schematically, the  $\pi$  exchange transition can be illustrated by Fig. 1, and the definition of kinematic parameters is the same as the previous subsection.

The transition matrix elements are as follows:

$$\begin{aligned}
T_{1fi} &= -i \left( \sqrt{2} g_{\pi NN} \frac{g_{Z\psi'\pi}}{M_Z} \frac{e}{f_{\psi'}} \right) \bar{u}(p_2) \gamma_5 u(p_1) \epsilon_Z^{*\mu} \epsilon^\nu [k_1 \cdot (k_2 - k_1) g_{\mu\nu} - k_{1\mu} (k_2 - k_1)_\nu] \\
&\times \frac{1}{q^2 - m_\pi^2} F_{\pi NN}(q^2) F_{Z\psi'\pi}(q^2),
\end{aligned} \tag{14}$$

which gives

$$\begin{aligned}
|\mathcal{M}|^2 &= \sum_{pol} |T_{1fi}|^2 \\
&= \left( \sqrt{2} g_{\pi NN} \frac{g_{Z\psi'\pi}}{M_Z} \frac{e}{f_{\psi'}} \right)^2 \frac{-q^2(q^2 - M_Z^2)^2}{(q^2 - m_\pi^2)^2} \left( \frac{\Lambda_\pi^2 - m_\pi^2}{\Lambda_\pi^2 - q^2} \right)^2 \left( \frac{M_{\psi'}^2 - m_\pi^2}{M_{\psi'}^2 - q^2} \right)^2. \quad (15)
\end{aligned}$$

One notices that the above equations have the same form as Eq. (11). This is because the longitudinal terms in  $Z\gamma\pi$  coupling vanish in the real photon limit for the chiral partner  $1^-$  and  $1^+$ .

The difference between these two parities leads to different values for the decay constant  $g_{Z\psi'\pi}$ . With the partial width:

$$\Gamma_{Z^+ \rightarrow \psi'\pi^+} = \left( \frac{g_{Z\psi'\pi}}{M_Z} \right)^2 \frac{|\mathbf{p}_{\pi cm}|}{24\pi M_Z^2} [2(p_\pi \cdot p_{\psi'})^2 + M_{\psi'}^2(m_\pi^2 + |\mathbf{p}_{\pi cm}|^2)], \quad (16)$$

we have

$$g_{Z\psi'\pi}/M_Z = 2.01 \text{ GeV}^{-1}, \quad (17)$$

which is smaller than that for  $1^-$ .

### C. Production of $Z(4430)$ with $J^P = 0^-$

If we take  $Z(4430)$  as a pseudoscalar meson with  $J^P = 0^-$ , the following effective lagrangian for  $Z\psi'\pi$  coupling is adopted:

$$\mathcal{L}_{Z\psi'\pi} = i g_{Z\psi'\pi} (\pi^- \partial_\mu Z^+ - \partial_\mu \pi^- Z^+) \psi'^\mu \quad (18)$$

Similarly, the  $\pi$  exchange transition can be illustrated in Fig. 1(a). The transition matrix element is as follows:

$$T_{fi} = i \left( \sqrt{2} g_{\pi NN} g_{Z\psi'\pi} \frac{e}{f_{\psi'}} \right) \bar{u}(p_2) \gamma_5 u(p_1) \frac{(q + k_2) \cdot \epsilon(k_1)}{q^2 - m_\pi^2} F_{\pi NN}(q^2) F_{Z\psi'\pi}(q^2) \quad (19)$$

which gives

$$\begin{aligned}
|\mathcal{M}|^2 &= \sum_{pol} |T_{fi}|^2 \\
&= \left( \sqrt{2} g_{\pi NN} \frac{g_{Z\psi'\pi}}{M_Z} \frac{e}{f_{\psi'}} \right)^2 \frac{-8q^2 M_Z^4}{(q^2 - m_\pi^2)^2} \left( \frac{\Lambda_\pi^2 - m_\pi^2}{\Lambda_\pi^2 - q^2} \right)^2 \left( \frac{M_{\psi'}^2 - m_\pi^2}{M_{\psi'}^2 - q^2} \right)^2. \quad (20)
\end{aligned}$$

Again, the coupling constant  $g_{Z\psi'\pi}$  is also determined by  $\Gamma_{Z^\pm \rightarrow \psi'\pi^\pm}$ :

$$\Gamma_{Z \rightarrow \psi'\pi} = \left( \frac{g_{Z\psi'\pi}}{M_Z} \right)^2 \frac{|\mathbf{p}_{\pi cm}|}{6\pi} \left[ \frac{(p_{\psi'} \cdot p_\pi)^2}{M_{\psi'}^2} - p_\pi^2 \right], \quad (21)$$

and we have

$$g_{Z\psi'\pi}/M_Z = 1.39 \text{ GeV}^{-1}. \quad (22)$$

Interestingly, the neutral  $Z^0 \rightarrow \psi'\pi^0$  has  $J^{PC} = 0^{--}$ , which is an exotic quantum number.

#### D. Numerical results for $\gamma p \rightarrow Z^+ n$

In Figs. 3, 4 and 5, the differential and total cross sections are plotted for  $J^P = 1^-, 1^+$ , and  $0^-$ , respectively. The photon energy for the differential cross sections is  $E_\gamma = 30$  GeV ( $W = 7.56$  GeV), which corresponds to the peaking energy region in the total cross sections. In all three cases, the forward peaking turns to be a prominent feature in the differential cross sections due to the pion exchange.

The results of Figs. 3, 4 and 5 show compatible production cross sections for those three spin-parity assignments. For spin-parity  $1^-$  and  $1^+$ , their production cross sections have the same expression in the real photon limit as noted before. The difference between Figs. 3 and 4 arises from the different coupling strengths for  $g_{Z\psi'\pi}$  extracted from  $Z^+ \rightarrow \psi'\pi^+$ .

The cross section for  $0^-$  production is found larger than the other two assignments. This is understandable by comparing Eqs. (11), (15), and (20) with each other. It also shows that in order to determine the quantum numbers, measurement of the angular distributions of  $Z \rightarrow \psi'\pi$  is necessary. For spin-parity  $1^+$ , the decay will be via relative  $S$ -wave between  $\psi'\pi$ , while it is via relative  $P$ -wave for  $1^-$  and  $0^-$ . Therefore, an observation of  $P$ -wave decay will require further studies such as polarization observables to determine the quantum numbers of  $Z(4430)$ .

For  $0^-$ ,  $a_0$  exchange is forbidden and the pion exchange is the exclusive leading contribution. For other  $J^P$   $a_0$  could contribute but in practice need not concern us here. Even were its coupling as large as that of the pion,  $g_{Z\psi'a_0} = g_{Z\psi'\pi}$ , its contribution to the cross-section is negligible (in Figs. 3 and 4, the results due to  $t$ -channel  $a_0$  exchanges are presented by the dotted curves). This in practise allows us to focus on the pion exchange mechanism in the photoproduction reaction as a reliable estimate of the lower bound of the production cross sections.

Due to the pion exchange the energy dependence of the total cross sections exhibits a strong threshold enhancement in  $\gamma p \rightarrow Z^+ n$ . It is similar to the charged  $\rho$  meson production near threshold where the charged pion exchange (unnatural parity exchange) also plays a dominant role [27, 28]. However, such a threshold enhancement seems to be absent in charmonium production, such as  $J/\psi$  and  $\psi'$  [29, 30]. This may be due to the dominance of the diffractive process which submerges the contributions from  $t$ -channel unnatural parity exchanges. Although  $J/\psi$  has a relatively large coupling to  $\rho\pi$ , whereby  $t$ -channel pion exchange turns to be important in  $\gamma p \rightarrow J/\psi p$ , the coupling is not as large as that for  $Z\psi'\pi$ . Consequently, the predicted threshold enhancement in  $Z$  meson photoproduction is strongly driven by the large  $Z\psi'\pi$  coupling.

Our main concern therefore is the possibility of some further contribution that is large and destructive. The most important question here seems to concern the role played by the intermediate  $J/\psi$  in the VMD model, which in a worst case could destructively interfere with the  $\psi'$ . By defining

$$\frac{\Gamma_{Z \rightarrow J/\psi \pi}}{\Gamma_{Z \rightarrow \psi' \pi}} \equiv x, \quad (23)$$

we include  $J/\psi$  contributions to the  $\pi$  exchange diagrams; i.e. the real photon couples to  $J/\psi$  and  $\psi'$ , which then couple to  $Z\pi$ . We then have

$$T_{fi} = T_{fi}^{\psi'} + T_{fi}^{J/\psi} = \left( 1 + \frac{g_{ZJ/\psi\pi}}{g_{Z\psi'\pi}} \frac{f_{\psi'}}{f_{J/\psi}} e^{i\theta} \right) T_{fi}^{\psi'} \quad (24)$$

where we have already set the form factors

$$F_{ZJ/\psi\pi}(q^2) = F_{Z\psi'\pi}(q^2) \quad (25)$$

for simplicity, and  $e^{i\theta}$  is the relative phase between the two transition matrix element. Couplings  $g_{ZJ/\psi\pi}$  and  $f_{J/\psi}$  can be determined by Eq. (2) and Eq. (6), respectively. The cross section becomes

$$\sigma_{\gamma p \rightarrow Z^+ n}^{J/\psi + \psi'} \simeq (1 + 0.75^2 x + 1.5\sqrt{x} \cos \theta) \sigma_{\gamma p \rightarrow Z^+ n}^{\psi'} \quad (26)$$

The worst destructive situation is at  $\theta = \pi$ . But the destructive effects will depend on the value of  $x$ . Note that Belle has not seen  $Z \rightarrow J/\psi\pi$  decay, which allows an estimate of  $x \leq 0.1$ , and with which the total cross section would be still sizeable.

If the  $Z$  meson is a genuine resonance, the threshold enhancement will be a signature for its existence. This can be further clarified by the study of background effects in  $\gamma p \rightarrow \psi'\pi^+ n$  in the next section.

### III. BACKGROUND ANALYSIS

Experimentally, the final state particles identified are  $\psi'$ ,  $\pi$  and nucleon. As a result, background contributions to the  $\psi'\pi N$  channel can interfere with the transitions we are interested in. As discussed earlier, one of the major contributions is due to the diffractive production of  $\psi'$  (Fig. 2). In this section, we combine  $\gamma p \rightarrow Z^+ n \rightarrow \psi'\pi^+ n$  and  $\gamma p \rightarrow \psi' p \rightarrow \psi'\pi^+ n$  together to make an estimate of the signal and background contributions. This could be useful for experimental search for the  $Z^+$  in this channel. Since the production rate for all these three spin-parities are similar, we only consider  $J^P = 1^-$  in the following analysis.

The schematic transition diagrams are illustrated in Fig. 2. We first extend the formulae of the previous section to  $\gamma p \rightarrow Z^+ n \rightarrow \psi'\pi^+ n$ , and then include the diffractive contributions from the Pomeron exchanges.

#### A. Meson exchange terms

By including the vertex coupling for  $Z^+ \rightarrow \psi'\pi^+$ , the transition amplitude for pion exchange can be explicitly written down

$$\begin{aligned}
T_{1fi}^{\mathcal{M}} &= \sum_{pol} \Gamma_{\gamma\psi'} \Gamma_{Z\psi'\pi}^1 \Gamma_{Z\psi'\pi}^2 \Gamma_{pn\pi} \times F_{Z\psi'\pi}(q_1^2) F_{\pi NN}(q_1^2) F_{Z\psi'\pi}(q_2^2) \\
&= -i \left[ \sqrt{2} g_{\pi NN} \frac{e}{f_{\psi'}} \left( \frac{g_{Z\psi'\pi}}{M_Z} \right)^2 \right] \bar{u}(p_3) \gamma_5 u(p_1) \epsilon_\mu(k) \epsilon_{\psi'}^\nu(q) \epsilon_{\mu_1\nu_1\alpha_1\beta_1} k^{\mu_1} q_2^{\alpha_1} \epsilon_{\mu_2\nu_2\beta_2} q^{\mu_2} q_2^{\alpha_2} \\
&\quad \times \frac{g^{\mu\nu_1} g^{\beta_1\beta_2}}{(q_1^2 - m_\pi^2)(q_2^2 - M_Z^2 + iM_Z\Gamma)} F_{Z\psi'\pi}(q_1^2) F_{\pi NN}(q_1^2) F_{Z\psi'\pi}(q_2^2), \tag{27}
\end{aligned}$$

where the vertex functions are

$$\Gamma_{\gamma\psi'} = \frac{eM_{\psi'}^2}{f_{\psi'}} \epsilon_\mu(k) \epsilon_{\psi'}^\mu(k) \tag{28}$$

$$\Gamma_{Z\psi'\pi}^1 = \frac{g_{Z\psi'\pi}}{M_Z} \epsilon_{\mu_1\nu_1\alpha_1\beta_1} k^{\mu_1} \epsilon_{\psi'}^{\nu_1}(k) q_2^{\alpha_1} \epsilon_Z^{\beta_1}(q_2) \tag{29}$$

$$\Gamma_{Z\psi'\pi}^2 = \frac{g_{Z\psi'\pi}}{M_Z} \epsilon_{\mu_2\nu_2\alpha_2\beta_2} q^{\mu_2} \epsilon_{\psi'}^{\nu_2}(q) q_2^{\alpha_2} \epsilon_Z^{\beta_2}(q_2) \tag{30}$$

$$\Gamma_{pn\pi} = -i\sqrt{2} g_{\pi NN} \bar{u}(p_3) \gamma_5 u(p_1), \tag{31}$$

and the form factor is

$$F_{Z\psi'\pi}(q_2^2) = \frac{\Lambda_Z^2 - M_Z^2}{\Lambda_Z^2 - q_2^2}. \tag{32}$$

Considering a moderate modification of the cutoff will not change the results significantly, we take  $\Lambda_Z = M_{\psi'}$  as an input value. The kinematic variables are denoted in Fig. 2.

#### B. Pomeron exchange term

Pomeron as a phenomenology accounting for the diffractive transitions has been widely studied in the literature [23, 24, 25]. In this approach, the Pomeron mediates the long range interaction between a confined quark and a nucleon, and has been shown to behave just like a  $C = +1$  isoscalar photon.

The Pomeron-nucleon coupling is determined by the vertex:

$$F_\mu(t) = 3\beta_0 \gamma_\mu f(t) \tag{33}$$

where  $t$  is the Pomeron momentum squared,  $\beta_0$  represents the coupling constants between a single Pomeron and a light constituent quark, and  $f(t)$  is the isoscalar nucleon electromagnetic form factor:

$$f(t) = \frac{4M_N^2 - 2.8t}{(4M_N^2 - t)(1 - t/0.7)^2} . \quad (34)$$

For the  $\gamma V \mathcal{P}$  vertex ( $V$  represents the corresponding vector meson, here is  $\psi'$ ), we take the on-shell approximation for restoring gauge invariance as [26]. Therefore the equivalent vertex for the  $\gamma \psi' \mathcal{P}$  is reduced to a loop tensor as follows:

$$\frac{2\beta_c \times 4\mu_0^2}{(M_{\psi'}^2 - t)(2\mu_0^2 + M_{\psi'}^2 - t)} T^{\mu\alpha\nu} , \quad (35)$$

where

$$T^{\mu\alpha\nu} = (k + q)^\alpha g^{\mu\nu} - 2k^\nu g^{\alpha\mu} \quad (36)$$

and  $\beta_c$  is the effective coupling constant between Pomeron and a charm quark within  $\psi'$ ;  $\mu_0$  is a cutoff of the form factor related to the Pomeron.

The amplitudes for Fig. 2(a) and (b) can then be expressed respectively as

$$T_{1fi}^{\mathcal{P}} = 24\sqrt{2}\beta_0\beta_c g_{\pi NN} \frac{\mu_0^2 f(t) \mathcal{G}_P(s, t)}{(M_{\psi'}^2 - t)(2\mu_0^2 + M_{\psi'}^2 - t)} T^{\mu\alpha\nu} \epsilon_{\psi'\nu}(q) \epsilon_\mu(k) \bar{u}(p_3) \gamma_5 \frac{\not{p}_2 + M_N}{p_2^2 - M_N^2} \gamma_\alpha u(p_1) \quad (37)$$

$$T_{2fi}^{\mathcal{P}} = 24\sqrt{2}\beta_0\beta_c g_{\pi NN} \frac{\mu_0^2 f(t) \mathcal{G}_P(s, t)}{(M_{\psi'}^2 - t)(2\mu_0^2 + M_{\psi'}^2 - t)} T^{\mu\alpha\nu} \epsilon_{\psi'\nu}(q) \epsilon_\mu(k) \bar{u}(p_3) \gamma_\alpha \frac{\not{p}'_2 + M_N}{p_2'^2 - M_N^2} \gamma_5 u(p_1) . \quad (38)$$

Function  $\mathcal{G}_P(s, t)$  is related to the Pomeron trajectory  $\alpha(t) = 1 + \epsilon + \alpha' t$  via

$$\mathcal{G}_P(s, t) = -i(\alpha' s)^{\alpha(t)-1} . \quad (39)$$

We also consider a form factor for the vertex  $pn\pi$  since the intermediate nucleon is off-shell, i.e.

$$F_{pn\pi}(s_{34}) = \frac{\Lambda_{pn\pi}^2 - M_N^2}{\Lambda_{pn\pi}^2 - s_{34}} \quad (40)$$

$$F_{pn\pi}(u_{14}) = \frac{\Lambda_{pn\pi}^2 - M_N^2}{\Lambda_{pn\pi}^2 - u_{14}} \quad (41)$$

where  $s_{34} = (p_3 + p_4)^2$ ,  $u_{14} = (p_1 - p_4)^2$ . Considering the kinematic region of the three-particles final state, we take a cutoff  $\Lambda_{pn\pi} = 1.0$  GeV in our following calculation to avoid the singularity.

### C. Numerical results with background contributions

Combining the signal terms and background amplitudes, the invariant transition amplitude becomes

$$\begin{aligned} |\mathcal{M}|^2 &= \sum_{pol} |T_{1fi}^{\mathcal{P}} + T_{2fi}^{\mathcal{P}} + T_{1fi}^{\mathcal{M}} + T_{2fi}^{\mathcal{M}}|^2 \\ &\equiv |A + B + C + D|^2 \\ &= |A|^2 + |B|^2 + |C|^2 + |D|^2 \\ &\quad + 2Re[AB^*] + 2Re[AC^*] + 2Re[AD^*] + 2Re[BC^*] + 2Re[BD^*] + 2Re[CD^*] . \end{aligned} \quad (42)$$

where  $2Re[CD^*] = 0$ , and  $2Re[AC^*]$ ,  $2Re[AD^*]$ ,  $2Re[BC^*]$ ,  $2Re[BD^*]$  are found to be much smaller than the other terms.



The following values are applied in the Pomeron exchange amplitudes:

$$\begin{aligned}\beta_0^2 &= 4.0 \text{ GeV}^2, \quad \beta_c^2 = 0.592 \text{ GeV}^2 \\ \alpha' &= 0.25 \text{ GeV}^{-2}, \quad \epsilon = 0.08, \quad \mu_0 = 1.2 \text{ GeV},\end{aligned}\tag{43}$$

where  $\beta_c$  is determined by considering the ratio  $\sigma_{\gamma p \rightarrow \psi' p} / \sigma_{\gamma p \rightarrow \psi p}$  through the Pomeron exchange. We take the following value H1 [30] as a constraint:

$$\frac{\sigma_{\gamma p \rightarrow \psi' p}}{\sigma_{\gamma p \rightarrow \psi p}} = 0.15.\tag{44}$$

With the coupling  $\beta_{c,J/\psi}^2 = 0.8 \text{ GeV}^2$  fixed by the  $J/\psi$  photoproduction [25], the coupling  $\beta_c$  for  $\psi'$  is determined. We note that these parameters lead to a reasonable description of both  $J/\psi$  and  $\psi'$  photoproduction in comparison with the experiment [31].

As shown by the total production cross section for  $\gamma p \rightarrow Z^+ n$ , the largest cross section is at  $W \simeq 8 \text{ GeV}$  ( $E_\gamma \simeq 34 \text{ GeV}$ ). We thus take this energy as an input to simulate the invariant mass spectrum for  $\gamma p \rightarrow \psi' \pi^+ n$ . This could be the kinematic region which favors the separation of the  $Z^+$  signals.

In Fig. 6, we calculate the total cross sections for  $\gamma p \rightarrow \psi' \pi^+ n$  including both signal and background contributions. As shown by the solid curve, the overall production cross section has a quick increase just above threshold and is dominated by the  $Z^+$  production as shown by the dotted curve. In contrast, the background contributions from the Pomeron exchange are relatively small and do not vary drastically with the increasing energies at  $W > 20 \text{ GeV}$ . This is consistent with the familiar diffractive behavior in vector meson photoproduction.

The steep rise of the cross section near threshold turns out to be very different from other known heavy vector photoproductions, such as  $\phi$ ,  $J/\psi$  and  $\psi'$ . In those cases, the threshold cross sections are rather smooth and no threshold enhancement has been observed. In the production of  $Z^+(4430)$ , its strong coupling to  $\psi' \pi$  gives rise to the predominant contributions from pion exchange. Note that  $\psi' \rightarrow e^+ e^-$  is also strong. These lead to an unusual prediction for its cross section near threshold.

It is more constructive to inspect the Dalitz plot for the three-body final state. We take a sample of the events at  $W = 8$  and  $12 \text{ GeV}$ , respectively. As shown by Fig. 7, a clear band appears in the invariant mass spectrum of  $\psi' \pi$  due to the  $Z$  resonance. Although we do not include the  $s$  and  $u$  channel nucleon resonances, their contributions seem not to demolish the  $Z(4430)$  band since their effects will add to the plot horizontally and in the low  $M_{n\pi}^2$  region, e.g.  $M_{n\pi}^2 < 5 \text{ GeV}^2$ .

With the increasing center-mass energy, the background from Pomeron-exchange becomes important, and the  $Z(4430)$  signals are submerged as shown by Fig. 8.

For the neutral  $Z^0(4430)$  production, the leading background contribution is the same as the charged  $Z$  production. In the  $t$ -channel  $Z^0$  production, an additional transition is the diffractive production of  $Z^0$  via Pomeron exchange for  $1^-$  or odderon exchange for  $1^+$ . It gives rise to two possibilities as shown in Fig. 9. In Fig. 9(a), the initial photon couples to the isoscalar component of a vector meson ( $c\bar{c}$ ), which then couples to  $Z^0$  by projecting the  $c\bar{c}$  component to the  $I = 1$  tetraquark wavefunction. Note that the exchange of Pomeron or odderon does not compensate the isospin. This process will be suppressed due to isospin violation. The other diffractive transition is that the initial photon couples to the isovector component of the intermediate meson as shown by Fig. 9(b). For the tetraquark scenario, the isovector component must be from the light  $q\bar{q}$  instead of  $c\bar{c}$ , hence requiring creation of a pair of  $c\bar{c}$  from the vacuum which then couples to the  $I = 1$  tetraquark wavefunction. Note that the  $c\bar{c}$  pair is much heavier than the light  $q\bar{q}$ . To form a tetraquark of  $cq\bar{c}\bar{q}$ , it needs a sizeable overlap between the final state  $Z^0$  and the intermediate isovector  $q\bar{q}$ . Since the  $c\bar{c}$  is much heavier than the light  $q\bar{q}$ , the  $Z^0$  wavefunction overlap with the  $c\bar{c}$  and light  $q\bar{q}$  should be small. This allows us to neglect the Pomeron or odderon exchange contributions to the direct  $Z^0$  production via diffractive processes. Due to the above argument, the neutral  $Z^0$  photoproduction turns out to be similar to the charged  $Z$  production studied earlier.

The neutral  $Z^0$  of  $0^-$  assignment leads to production of exotic quantum number  $0^{--}$ . If indeed the  $Z^0(4430) \rightarrow \psi' \pi^0$  has a partial width of  $\sim 45 \text{ MeV}$ , its photoproduction cross section near threshold will also be significant. By measuring the angular distribution of  $Z^0 \rightarrow \psi' \pi^0$ , its quantum numbers can also be determined.

#### IV. CONCLUSION

In this work we have made a detailed analysis of the photoproduction reaction  $\gamma p \rightarrow Z^+(4430)n$  in an effective Lagrangian approach for possible assignments of  $J^P = 1^-, 1^+$  and  $0^-$  to the  $Z^0(4430)$ . As suggested by the observation of Belle, we show that the  $t$ -channel pion exchange is an important production mechanism for creating  $Z^+(4430)$  at the rate of several tens of nano-barn. In this process the  $\pi NN$  coupling can be well constrained and the  $Z\gamma\pi$  coupling can be extracted from the  $Z\psi'\pi$  data via VMD model.

We have also checked the possible effect of  $t$ -channel  $a_0$  exchange. We find its contributions are relatively small even if, as an upper limit, we fix the  $Z\psi'a_0$  coupling to be the same as  $g_{Z\psi'\pi}$ . Since there is no interference between the  $a_0$  and pion exchange amplitudes, we can neglect the  $a_0$  exchange in the calculation and only adopt the relatively well-defined pion exchange for estimating the lower bound of the  $Z(4430)$  photoproduction cross sections. We find that due to pion exchange, a clear threshold enhancement is predicted for  $Z(4430)$  photoproduction, which is different from photoproduction of  $J/\psi$  and  $\psi'$  near threshold, and could be a signature for the  $Z(4430)$  existence. This is also the kinematic region that uncertainties arising from other unknown processes can be overlooked as a reasonable approximate.

We also consider possible background contributions to the signals in  $\gamma p \rightarrow \psi'\pi^+n$ , where the diffractive production of  $\psi'$  turns to be the leading source. Interestingly, it shows that the interferences from the background terms are rather small. In the Dalitz plot at  $W = 8$  GeV ( $E_\gamma \simeq 34$  GeV), a clear band of the  $Z$  meson signals appear in the invariant mass spectrum of  $\psi'\pi$ . Similar results are obtained for the neutral production channel. For other background contributions from diffractive transitions, we argue that they may be suppressed by isospin conservation and momentum mismatching. Although nucleon resonance contributions to the background in Fig. 2(A) and (B) have not been included in this calculation, their effects are unlikely to submerge the  $Z(4430)$  band in the Dalitz plot. The reason is that the nucleon resonance cross sections will accumulate horizontally in a form of uneven bands, and be located at  $M_{n\pi}^2 < 5$  GeV<sup>2</sup>. In the kinematics of higher  $M_{n\pi}^2$  interferences from the nucleon resonances are expected to be negligible. As a consequence, the  $Z(4430)$  production signals can be rather cleanly isolated from the background, and the measurement of the angular distributions between  $\psi'$  and  $\pi$  will tell whether they are in a relative  $S$  or  $P$  wave. The quantum numbers of the  $Z(4430)$  can thus be determined.

In summary, in order to establish the  $Z(4430)$  as a concrete candidate of tetraquark state and determine its quantum numbers, further search for its signals in other production processes is necessary. Supposing it is a genuine resonance with sizeable partial decay width to  $\psi'\pi$  [1], we have argued that photoproduction should be useful for providing a clear and consistent evidence for its existence. Experimental data which have been collected at H1 and ZEUS may already contain such information.

#### Acknowledgement

Useful discussion with ZhiQing Zhang about experiments at HERA is acknowledged. This work is supported, in part, by the U.K. EPSRC (Grant No. GR/S99433/01), National Natural Science Foundation of China (Grant No.10675131), and Chinese Academy of Sciences (KJCX3-SYW-N2). F.E.C. acknowledges support from the U.K. Science and Technology Facilities Council (STFC) and the EU-RTN programme contract No. MRTN-CT-2006-035 482: "Flavianet".

#### Appendix

We give below the details for  $a_0$  exchange.

### A. $J^P = 1^-$

The Lagrangian for the  $Z\psi'a_0$  is:

$$\mathcal{L}_{Z\psi'a_0} = \frac{g_{Z\psi'a_0}}{M_Z} (\partial^\alpha Z^\beta \partial_\alpha \psi'_\beta - \partial^\alpha Z^\beta \partial_\beta \psi'_\alpha) a_0, \quad (45)$$

where  $g_{Z\psi'a_0}$  is the coupling constant. At this moment, no information about this coupling is available. A conservative estimate is to set it the same as  $g_{Z\psi'\pi}$  as an upper limit.

The Lagrangian for  $a_0 NN$  interaction is

$$\begin{aligned} \mathcal{L}_{a_0 NN}^{int} &= g_{a_0 NN} \bar{N}(\vec{\tau} \cdot \vec{a}_0) N \\ &= g_{a_0 NN} (\bar{p} p a_0 + \sqrt{2} \bar{p} n a_0 + \sqrt{2} \bar{n} p a_0 - \bar{n} n a_0), \end{aligned} \quad (46)$$

where  $g_{a_0 NN}^2/4\pi = 1.075$  is adopted. A form factor is also applied

$$F_{a_0 NN} = \frac{\Lambda_{a_0}^2 - m_{a_0}^2}{\Lambda_{a_0}^2 - q^2}, \quad (47)$$

with  $\Lambda_{a_0} = 2.0$  GeV [16, 19].

The amplitude for  $a_0$  exchange is:

$$\begin{aligned} T_{2fi} &= \left( \sqrt{2} g_{a_0 NN} \frac{g_{Z\psi'a_0}}{M_{\psi'}} \frac{e}{f_{\psi'}} \right) \bar{u}(p_2) u(p_1) k_2^\alpha (k_{1\alpha} g_{\mu\beta} - k_{1\beta} g_{\mu\alpha}) \epsilon_Z^{*\beta} \epsilon^\mu \\ &\times \frac{1}{q^2 - m_{a_0}^2} F_{a_0 NN}(q^2) F_{Z\psi'a_0}(q^2). \end{aligned} \quad (48)$$

### B. $J^P = 1^+$

For the production of  $Z(4430)$  with  $J^P = 1^+$ , its difference from  $J^P = 1^-$  is at the  $Z\psi'\pi$  and  $Z\psi'a_0$  vertices for which the following effective lagrangians are adopted [21, 22]:

$$\mathcal{L}_{Z\psi'\pi} = \frac{g_{Z\psi'\pi}}{M_Z} (\partial^\alpha \psi'^\beta \partial_\alpha \pi Z_\beta - \partial^\alpha \psi'^\beta \partial_\beta \pi Z_\alpha), \quad (49)$$

$$\mathcal{L}_{Z\psi'a_0} = \frac{g_{Z\psi'a_0}}{M_Z} \varepsilon_{\mu\nu\alpha\beta} \partial^\mu \psi'^\nu \partial^\alpha Z^\beta a_0, \quad (50)$$

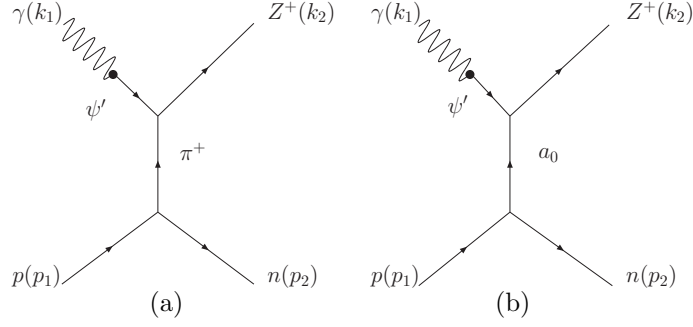
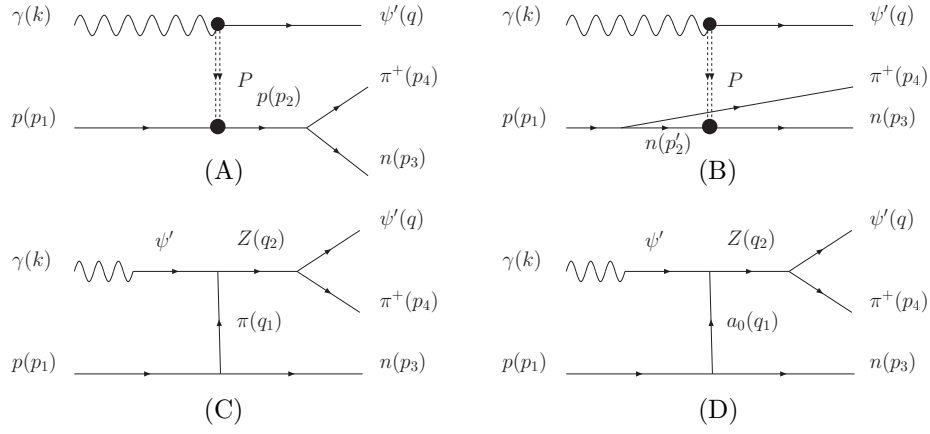
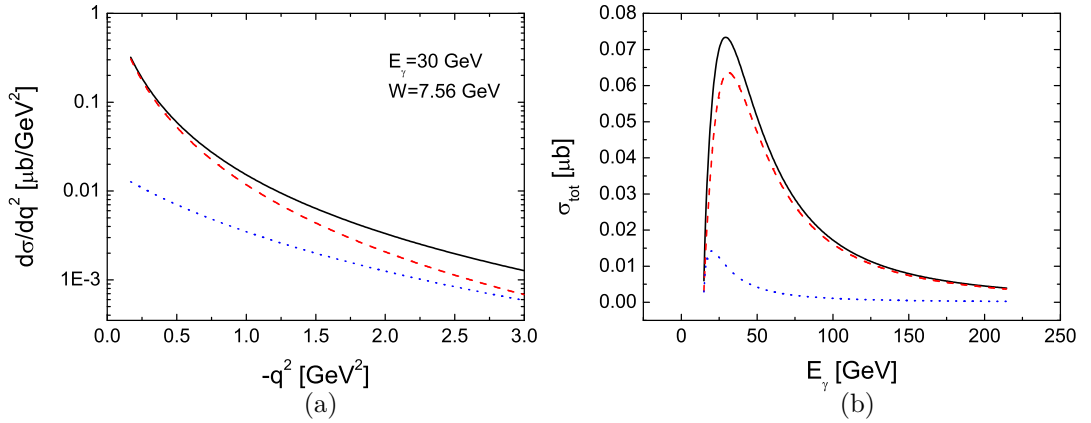
where the notations are the same as Eq. (1).

The transition matrix elements are as follows:

$$\begin{aligned} T_{2fi} &= \left( \sqrt{2} g_{a_0 NN} \frac{g_{Z\psi'a_0}}{M_Z} \frac{e}{f_{\psi'}} \right) \bar{u}(p_2) u(p_1) \varepsilon_{\mu\nu\alpha\beta} k_1^\mu k_2^\alpha \epsilon_Z^{*\nu} \epsilon^{*\beta} \\ &\times \frac{1}{q^2 - m_{a_0}^2} F_{a_0 NN}(q^2) F_{Z\psi'a_0}(q^2). \end{aligned} \quad (51)$$

- 
- [1] K. Abe *et al.* [Belle Collaboration], arXiv:0708.1790[hep-ex].
  - [2] L. Maiani, F. Piccinini, A. D. Polosa and V. Riquer, Phys. Rev. **D 71**, 014028 (2005).
  - [3] L. Maiani, V. Riquer, F. Piccinini and A. D. Polosa, Phys. Rev. **D 72**, 031502 (2005).
  - [4] L. Maiani, A.D. Polosa and V. Riquer, arXiv:0708.3997[hep-ph].
  - [5] I. Bigi, L. Maiani, F. Piccinini, A. D. Polosa and V. Riquer, Phys. Rev. **D 72**, 114016 (2005).
  - [6] J. L. Rosner, Phys. Rev. **D 69**, 094014 (2004).

- [7] J.L. Rosner, arXiv:0708.3496[hep-ph].
- [8] J.L. Rosner, Phys. Rev. **D 74**, 076006 (2006).
- [9] D.V. Bugg, arXiv:0709.1254[hep-ph].
- [10] C. Meng and K.-T. Chao, arXiv:0708.4222[hep-ph].
- [11] See a recent review, F.E. Close, arXiv:0801.2646[hep-ph].
- [12] N. A. Tornqvist, Phys. Lett. B **590**, 209 (2004) [arXiv:hep-ph/0402237].
- [13] F.E. Close and P.R. Page, Physics Letters **B578** 119 (2004)
- [14] E. S. Swanson, Phys. Lett. B **588**, 189 (2004) [arXiv:hep-ph/0311229].
- [15] F.E. Close and H.J. Lipkin, Phys. Rev. Lett. **41**, 1263 (1978).
- [16] B. Friman and M. Soyeur, Nucl. Phys. A **600**, 477 (1996).
- [17] W. M. Yao *et al.* [Particle Data Group], J. Phys. G **33** 1 (2006).
- [18] M. L. Goldberger and S. B. Treiman, Phys. Rev. **110**, 1178 (1958).
- [19] M. Kirchbach, D. O. Riska, Nucl. Phys. A **594**, 419 (1995).
- [20] T.E.O. Ericson and M. Rosa-Clot, Nucl. Phys. **A 405**, 497 (1983); K. Holinde, Phys. Rep. **68**, 121 (1981).
- [21] L. Xiong, Edward V. Shuryak, and G. E. Brown, Phys. Rev. D **46**, 3798 (1992).
- [22] K. Haglin, Phys. Rev. C **50**, 1688 (1994).
- [23] A. Donnachie and P. V. Landshoff, Phys. Lett. B **185**, 403 (1987).
- [24] M. A. Pichowsky and T. S. H. Lee, Phys. Lett. B **379**, 1 (1996) [arXiv:nucl-th/9601032]
- [25] J. M. Laget, and R. Mendez-Galain, Nucl. Phys. A **581**, 397 (1995)
- [26] Q. Zhao, J. P. Didelez, M. Guidal, and B. Saghai, Nucl. Phys. A **660**, 323 (1996).
- [27] T.H. Bauer, R.D. Spital, D.R. Yennie, and F.M. Pipkin, Rev. Mod. Phys. **50**, 261 (1978).
- [28] Q. Zhao, Z.-P. Li and C. Bennhold, Phys. Rev. C **58**, 2393 (1998).
- [29] C. Adloff *et al.* [H1 Collaboration], Phys. Lett. **B 483**, 23 (2000).
- [30] C. Adloff *et al.* [H1 Collaboration], Phys. Lett. **B421**, 385 (1998).
- [31] H. Jung, arXiv:0801.1970[hep-ex].

FIG. 1:  $Z$  production through meson exchangeFIG. 2: Major processes that contribute to the background in  $\gamma p \rightarrow \psi' \pi^+ n$ .FIG. 3: Differential and total cross sections for  $\gamma p \rightarrow Z^+ n$  where the spin-parity of  $Z$  is  $J^P = 1^-$ . The dashed and dotted lines denote the  $\pi$  and  $a_0$ -exchange contributions, respectively, and the solid line is the sum of both.

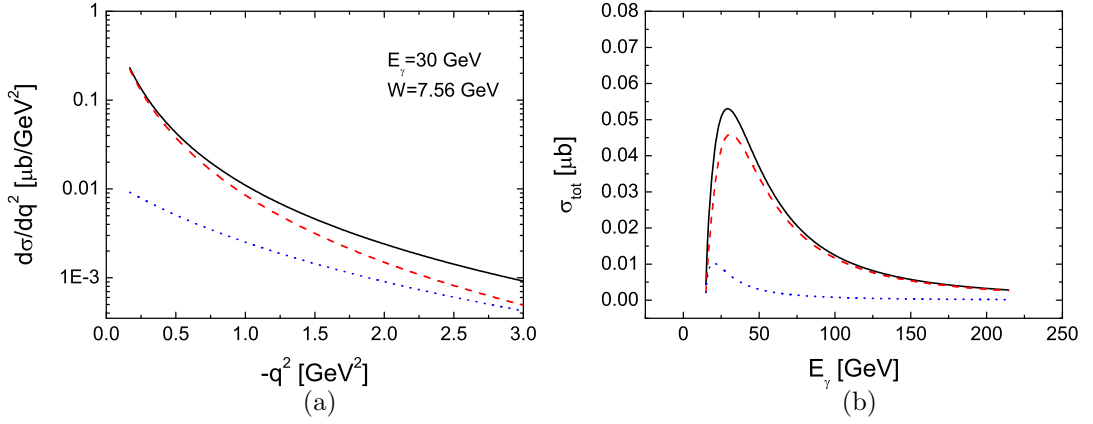


FIG. 4: Differential and total cross sections for  $\gamma p \rightarrow Z^+ n$  where the spin-parity of  $Z$  is  $J^P = 1^+$ . The notations are the same as Fig. 3.

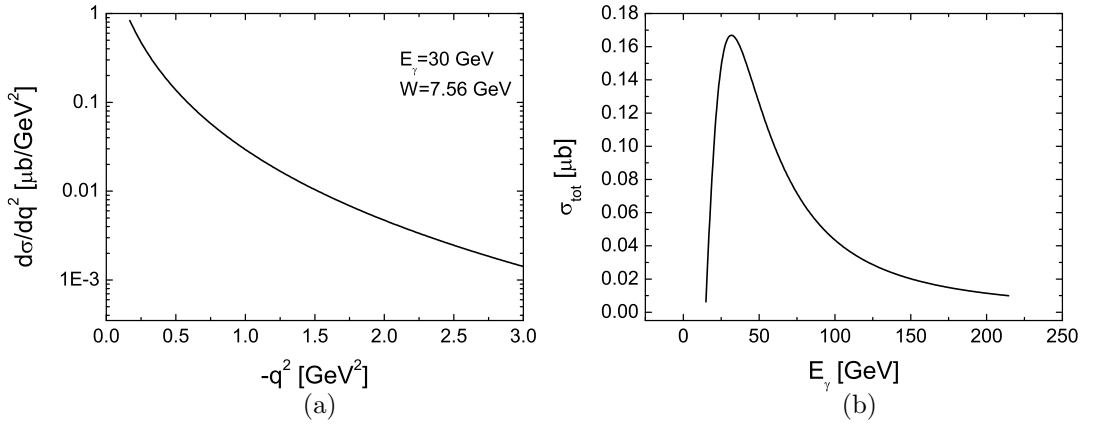


FIG. 5: Differential and total cross section for  $\gamma p \rightarrow Z^+ n$  through  $\pi$ -exchange where the spin-parity of  $Z$  is  $J^P = 0^-$ .

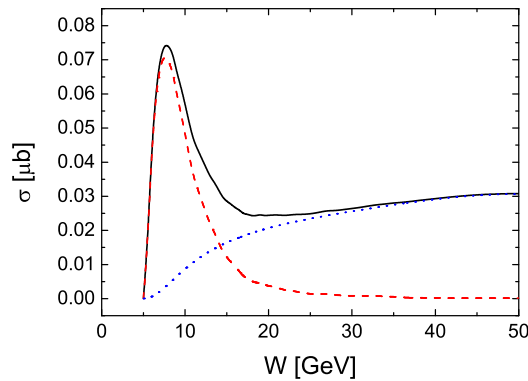


FIG. 6: Energy dependence of total cross section for  $\gamma p \rightarrow \psi' \pi^+ n$ .  $W$  is the c.m. energy. The dashed line denotes the meson ( $\pi$  and  $a_0$ ) exchange contribution, the dotted line is the Pomeron-exchange contribution, and the solid line is the full contribution.

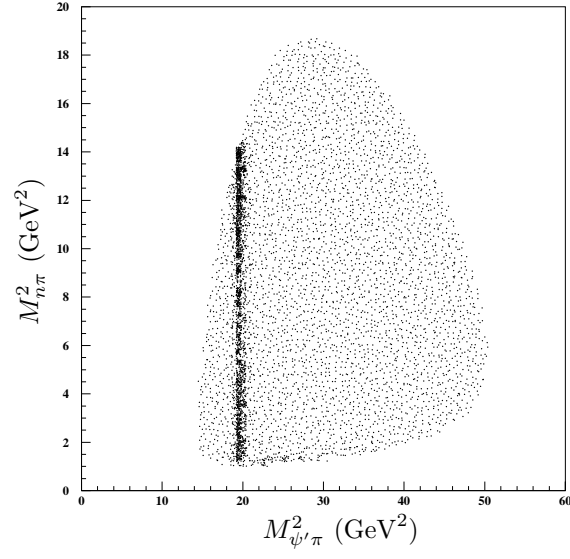


FIG. 7: Dalitz plot of  $\gamma p \rightarrow n\psi'\pi^+$  at  $W = 8$  GeV ( $E_\gamma \simeq 34$  GeV). The axial variables are  $M_{\psi'\pi}^2 = (q + p_4)^2$ , and  $M_{n\pi}^2 = (p_3 + p_4)^2$ .

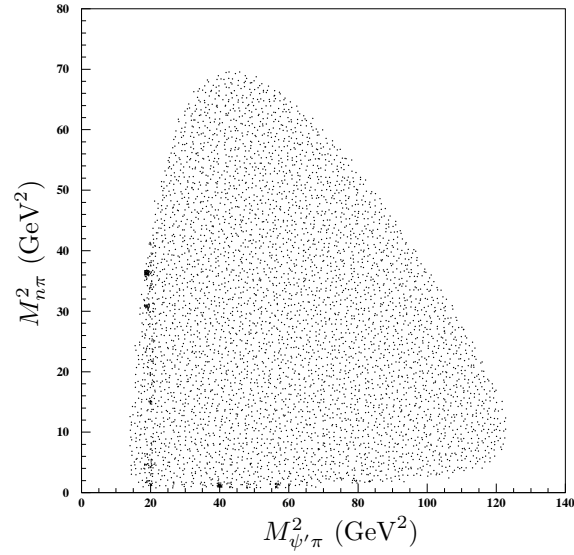


FIG. 8: Dalitz plot of  $\gamma p \rightarrow n\psi'\pi^+$  at  $W = 12$  GeV ( $E_\gamma \simeq 76$  GeV). The axial variables are the same as Fig. 7.

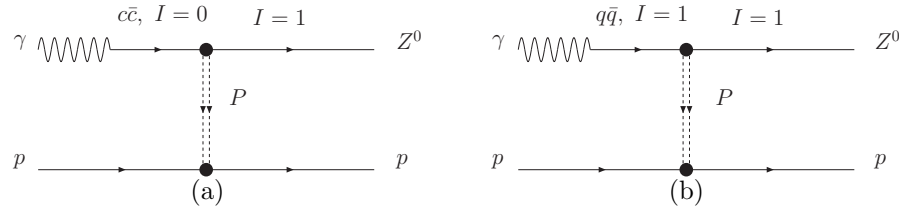


FIG. 9: Schematic diagrams for the diffractive production of  $Z^0(4430)$  in  $\gamma p \rightarrow Z^0 p$ . Figure (a) and (b) illustrate subprocesses for producing  $Z^0$  via intermediate  $I = 0$  and  $I = 1$  vector meson components in the VMD model.